AIP | Applied Physics
Letters

Gap length effect on electron energy distribution in capacitive radio frequency discharges

S. J. You, S. S. Kim, Jung-Hyung Kim, Dae-Jin Seong, Yong-Hyeon Shin et al.

Citation: Appl. Phys. Lett. **91**, 221501 (2007); doi: 10.1063/1.2805032
View online: http://dx.doi.org/10.1063/1.2805032
View Table of Contents: http://apl.aip.org/resource/1/APPLAB/v91/i22
Published by the American Institute of Physics.

APPLIED PHYSICS LETTERS **91**, 221501 (2007)

Gap length effect on electron energy distribution in capacitive radio frequency discharges

S. J. You
Center for Vacuum Technology, Korea Research Institute of Standards and Science, Daejeon 305-306, Korea

S. S. Kim
National Fusion Research Institute, Daejeon 305-333, Korea

Jung-Hyung Kim,[a] Dae-Jin Seong, and Yong-Hyeon Shin
Center for Vacuum Technology, Korea Research Institute of Standards and Science, Daejeon 305-306, Korea

H. Y. Chang
Department of Physics, Korea Advanced Institute of Science and Technology, Daejeon 305-701, Korea

(Received 19 September 2007; accepted 12 October 2007; published online 26 November 2007)

A study on the dependence of electron energy distribution function (EEDF) on discharge gap size in capacitive rf discharges was conducted. The evolution of the EEDF over a gap size range from 2.5 to 7 cm in 65 mTorr Ar discharges was investigated both experimentally and theoretically. The measured EEDFs exhibited typical bi-Maxwellian forms with low energy electron groups. A significant depletion in the low energy portion of the bi-Maxwellian was found with decreasing gap size. The results show that electron heating by bulk electric fields, which is the main heating process of the low-energy electrons, is greatly enhanced as the gap size decreases, resulting in the abrupt change of the EEDF. The calculated EEDFs based on nonlocal kinetic theory are in good agreement with the experiments. © *2007 American Institute of Physics*. [DOI: 10.1063/1.2805032]

Radio frequency capacitive discharge is widely used in material processing because it can easily produce reactive radicals at low temperature.[1] In various low-temperature plasma processes including polyetch, metal-etch, oxide-etch, etch-back processes, and deposition, the radicals are known to be key players influencing the process results. The absolute values of radical densities are closely related to the etch and deposition rates, while the relative density ratios of the radicals determine the etch selectivity and film deposition quality.[2] For example, CF_2 radical is known as the main precursor of fluorocarbon film deposition on silicon or silicon nitride during dielectric etching with fluorocarbon plasmas. The film suppresses silicon etching and increases the etching selectivity of oxide to silicon. On the other hand, F radical etches both silicon and oxide. In this case, it is essential to control density ratio between CF_2 and F to achieve a satisfactory etching selectivity.[3]

Since primary reactions creating the radicals are electron-impact dissociations of parent molecules in the gas phase, the composition of the radicals is predominantly governed by the number of electrons above the dissociation threshold energies in an energy space, i.e., electron energy distribution. Therefore, in order to control the plasma process and to improve the device performance, one should first examine the effect of changing external parameter on electron energy distribution.[4] There have been many informative studies on the dependence of the electron energy distribution function (EEDF) on external parameters, such as gas pressure,[5] discharge current,[6] driving frequency,[7] and magnetic field.[8,9]

In this letter, the discharge gap size effect on the EEDF formation is investigated. We will present EEDFs measured and calculated at various gap lengths in capacitive rf discharges. The EEDFs at large gap sizes show typical bi-Maxwellian forms characterized by two distinctive electron groups with different temperatures. As the gap size decreases, the distinction between the two energy groups in the bi-Maxwellian becomes weak with a number of low energy electrons disappearing. This indicates that the low energy electrons are effectively heated at small gap size.

The experiment was performed in a capacitive reactor described in Ref 10. To acquire the EEDFs, the ac signal superpositio method and rf compensated Langmuir probe were used.[11] The EEDF measurement was performed at 65 mTorr and 1 A while the gap length changed from 7 cm to 2.5 cm.

The experimental results are presented in Fig. 1. The EEPFs show bi-Maxwellian distributions with low energy electron groups caused by nonlocal electron kinetics. The observed bi-Maxwellian structure is consistent with the previous measurements at similar conditions to this experiment.[5,6] It can be characterized by a low-temperature low energy electron group and a high-temperature high energy electron group. According to the nonlocal electron kinetics, the electrons with energy higher than dc ambipolar potential can reach the sheath region where the stochastic heating takes place, thereby being strongly heated through interactions with moving sheath. On the contrary, the low energy electrons, which cannot overcome the dc potential, are heated only by bulk electric fields. Since the rf power transfer to electrons through the bulk heating process is normally much lower than that through the stochastic heating process, the temperature of the low energy electrons is lower

---

[a] Electronic mail: jhkim86@kriss.re.kr.

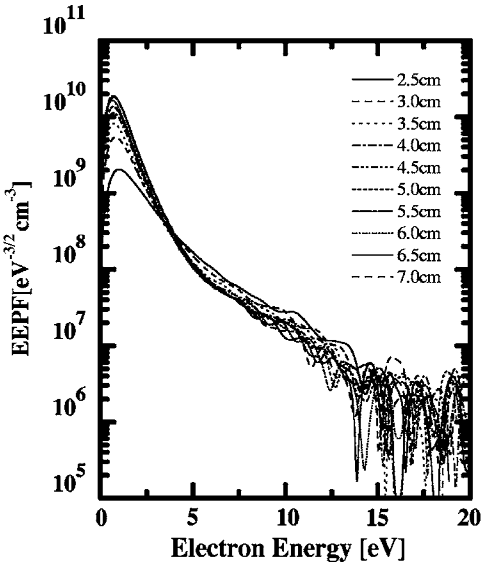

FIG. 1. Measured EEPFs for various gap lengths at 65 mTorr and 1 A.

compared to the high energy electrons. The distinction between the two energy groups is more intensified in Ramsauer gas discharges such as Ar discharges, due to lower collision frequency at lower energy.[5]

As the discharge gap length (L) decreases, the difference between the two groups becomes obscure, as shown in Fig. 1. Particularly, in the small gap size range of $L \leqslant 3.5$ cm, the EEPF changes considerably with electrons escaping the low energy region. The electron density of the low energy group decreases from 6.9×10^{10} to 6×10^{9} cm^{-3} and the electron temperature increases from 0.62 to 1.1 eV, while the high energy group varies slightly with density from 2.9×10^{8} to 5.5×10^{8} cm^{-3} and temperature from 3.5 to 3.3 eV, as the gap length decreases from 7 to 2.5 cm. This change of EEDF shows that the heating efficiency of the low energy electron group by the bulk electric fields is enhanced with decreasing gap size.

To theoretically examine the mechanism for this efficient low energy electron heating with different gap sizes, we solved the following Fokker-Planck equation:[12]

$$\frac{1}{v}\frac{d}{d\epsilon}v\left[(D_\epsilon + D_{ee} + D_{\mathrm{en}})\frac{df_e}{d\epsilon} + (V_{ee} + V_{\mathrm{en}})f_e\right] = I, \qquad (1)$$

where D_ϵ is the energy diffusion coefficient describing the electron heating by the bulk electric field and moving sheaths, $D_{ee(n)}$ and $V_{ee(n)}$ are the coefficients of diffusion and dynamical friction caused by electron-electron (neutral) collisions, and I represents inelastic collisions including ionization and excitation. Recently, the energy diffusion coefficient was calculated for a semi-infinite plasma.[13] We extended the theory in Ref. 13 to a finite plasma case and the result is given as

$$D_\epsilon = \frac{\epsilon}{2m_e}\,\mathrm{Re}\sum_n i\int_{-1}^{1}\frac{|-eE_n + 2m_eL^{-1}V_{\mathrm{sh}}v_z'\Theta(|v_z| - u_{\mathrm{sh}})|^2}{(\omega + i\nu_{\mathrm{en}} - k_nv_z)} \times t^2 dt, \qquad (2)$$

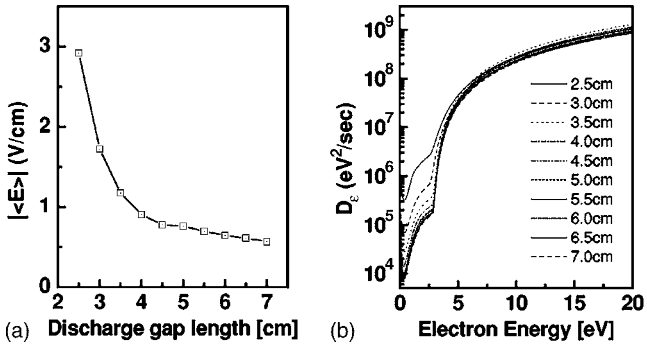

FIG. 2. (a) Spatially averaged electric field strength $|\langle E\rangle|$ as a function of L and (b) electron energy diffusion coefficients for various discharge gap lengths.

where E_n is the nth Fourier component of the bulk electric field $(E=\Sigma_n E_n e^{ik_nz}, k_n = n\pi/L)$, V_{sh} is the velocity of the moving sheath, v_z' is the axial component of electron velocity in the sheath $(v_z'^2 = v_z^2 - u_{\mathrm{sh}}^2)$, $u_{\mathrm{sh}} = \sqrt{2e\phi_b/m_e}$ with ϕ_b being a dc ambipolar barrier potential, Θ is the Heaviside step function, $\omega = 2\pi\nu_{\mathrm{rf}}$ and $t = v_z/v$. The summation in Eq. (2) is performed for odd integers. Neglecting conduction currents and assuming a uniform density n_{sh} inside the sheath region, the velocity of the moving sheath is given by $V_{\mathrm{sh}} = -J_0/en_{\mathrm{sh}}$, where J_0 is a rf discharge current density through the bulk plasma.[14–17] The electric field can be determined from current conservation in a similar way as that in Ref. 13 and is given by

$$E_n = \frac{(1-\chi_n)J_n}{\sigma_n - i\omega/4\pi}, \qquad (3)$$

where $J_n = -(2i/n\pi)J_0$ is the Fourier component of the rf discharge current density,

$$\sigma_n = -\frac{ie^2}{4\pi}\left(\frac{m_e}{2}\right)^{1/2}\int \frac{v_z}{\omega + i\nu_{\mathrm{en}} - k_nv_z}\frac{\partial f_e}{\partial v_z}d^3\mathbf{v}, \qquad (4)$$

$$\chi_n = \frac{k_n}{2\pi n_{\mathrm{sh}}}\left(\frac{m_e}{2}\right)^{3/2}\int \frac{v_zv_z'\Theta(|v_z| - u_{\mathrm{sh}})}{\omega + i\nu_{\mathrm{en}} - k_nv_z}\frac{\partial f_e}{\partial v_z}d^3\mathbf{v}. \qquad (5)$$

Details of the derivation for the above results will be presented elsewhere.

The calculation results for E, D_ϵ, and f_e under the same conditions as in the experiment are presented in Figs. 2 and 3. Here, we used the measured EEPFs in Fig. 1 when calculating σ_n and χ_n. According to Ref. 18, the ambipolar potential ϕ_b and sheath characteristics are closely related to the high energy electron temperature (T_1). However, it is very difficult and complicated problem to find an exact relationship between them. In this work, to avoid complexity, we used an "ansatz" $\phi_b = AT_1$ with a constant A and adapted $A = 0.8$ as a value to give calculation results closest to experiments. Figure 2(a) shows the magnitude of spatially averaged electric field at various gap lengths. As stated before, the electric field strength increases with decreasing gap length. In Fig. 2(b), the energy diffusion coefficients corresponding to the electric fields in Fig. 2(a) are plotted. The abrupt increase of D_ϵ starts from $\epsilon = e\phi_b$ by the inclusion of a stochastic sheath heating term. For low energy electrons of $\epsilon < e\phi_b$, D_ϵ in Eq. (2) depends only on the bulk electric field E. In Figs. 2(a) and 2(b), we can see that D_ϵ in the low energy region increases as E increases.

Figure 3 shows the calculated EEPFs using D_ϵ in Fig. 2(b) and measured densities. The EEPFs in Fig. 3 are qualitatively well consistent with the experimental results in Fig. 1. As the gap length decreases, the population of low energy electrons diminishes. Coincidently with the experiments, the

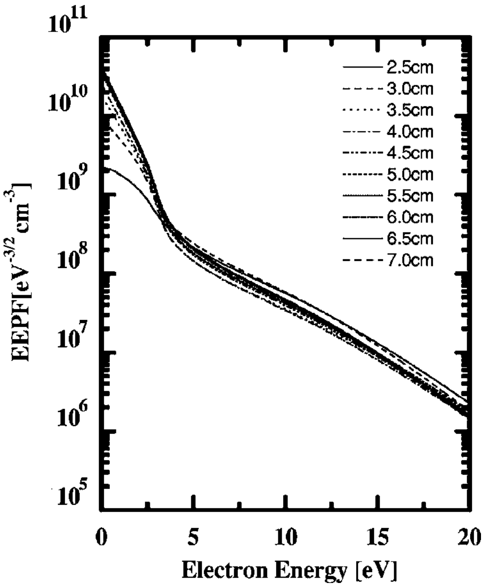

FIG. 3. Calculated EEPFs for various discharge gap lengths at 65 mTorr and 1 A.

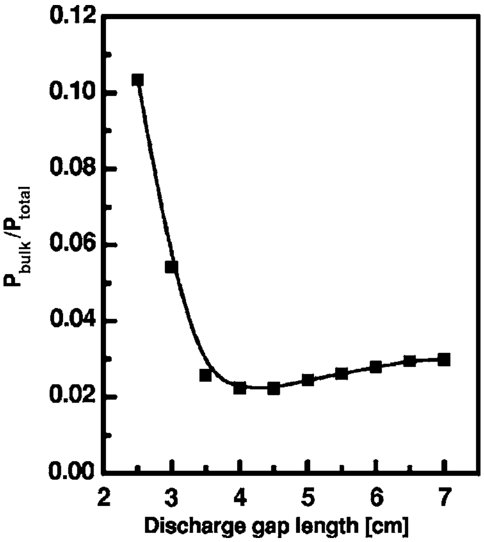

FIG. 4. Gap length dependence of $P_{\rm bulk}/P_{\rm tot}$.

change of the EEPFs is considerable in the range of $L \leqslant 3.5$ cm. This is ascribed to the increase of D_ϵ in the low energy region accompanied by the bulk electric field enhancement, as mentioned in Fig. 2.

In order to estimate the degree of the bulk fraction of electron heating, we calculated a power density ratio $P_{\rm bulk}/P_{\rm tot}$ as a function of L, where $P_{\rm tot}=-\int_0^\infty \epsilon^{1/2} D_\epsilon (df_e/d\epsilon) d\epsilon$ is the total absorbed power density and $P_{\rm bulk}=-\int_0^\infty \epsilon^{1/2} D_{\epsilon,\rm bulk} (df_e/d\epsilon) d\epsilon$ represents absorbed power density only through the bulk electric fields. Here, we defined $D_{\epsilon,\rm bulk}$ as D_ϵ with $V_{\rm sh}=0$ in Eq. (2) and used the measured EEPFs in Fig. 1. The results are plotted in Fig. 4, where one can see that the power absorption through the bulk heating process increases dramatically while decreasing L for $L \leqslant 3.5$ cm. A similar result, discharge power absorption increases with decreasing discharge gap influencing the EEDFs, has been found in inductively coupled discharge, but the result originated from the electron bounce resonance, not from the enhancement of collisional heating in the bulk.[19]

In conclusion, through the EEDF measurement of a low-pressure capacitive Ar discharge, we observed the efficient heating for low energy electrons induced by the gap size effect. The low energy electrons, which are unable to interact with moving sheath, are heated only by bulk electric fields. It is shown that the reduction of the gap size raises the bulk electric field strength and, accordingly, enhances the low energy electron heating. The calculated EEDFs based on the kinetic theory are in good agreement with the experiments.

This work was sponsored in part by the SYSTEM I.C. 2010 of the Ministry of Science and Technology (MOST) and the Ministry of Commerce, Industry and Energy (MOCIE) and by a grant from the Interdisciplinary Research Program of KOSEF. It was also supported in part by the National Research Laboratory Project of Korea (M1-0104-00-0071) and Tera Level Nanodevices Project of MOST (TND, Grant No. M101KC010015-03K0301-01520). One of the authors would like to thank PLASMART Inc. for its technical and financial support for this work.

[1] B. Chapman, *Glow Discharge Processes* (Wiley, New York, 1980).
[2] C. Kang (private communication).
[3] S. Samukawa, Jpn. J. Appl. Phys., Part 1 **33**, 2133 (1994).
[4] H. Sugai, I. Ghanashev, M. Hosokawa, K. Mizuno, K. Nakamura, H. Toyoda, and K. Tamauchi, Plasma Sources Sci. Technol. **10**, 378 (2001).
[5] V. A. Godyak and R. B. Piejak, Phys. Rev. Lett. **65**, 996 (1990).
[6] U. Buddemeier, U. Kortshagen, and I. Pukropski, Appl. Phys. Lett. **67**, 191 (1995).
[7] E. A. Fattah and H. Sugai, Appl. Phys. Lett. **83**, 1533 (2003).
[8] M. M. Turner, D. A. W. Hutchinson, R. A. Doyle, and M. B. Hopkins, Phys. Rev. Lett. **76**, 2069 (1996).
[9] D. A. W. Hutchinson, M. M. Turner, R. A. Doyle, and M. B. Hopkins, IEEE Trans. Plasma Sci. **23**, 636 (1995).
[10] S. J. You, C. W. Chung, K. H. Bai, and H. Y. Chang, Appl. Phys. Lett. **81**, 2529 (2002).
[11] S. J. You, S. S. Kim, and H. Y. Chang, Appl. Phys. Lett. **85**, 4872 (2004).
[12] S. S. Kim, C. W. Chung, and H. Y. Chang, Thin Solid Films **435**, 72 (2003).
[13] I. D. Kaganovich, Phys. Rev. Lett. **89**, 265006 (2002).
[14] U. Kortshagen, C. Busch, and L. D. Tsendin Plasma Sources Sci. Technol. **5**, 1 (1996).
[15] I. D. Kaganovich and L. D. Tsendin, IEEE Trans. Plasma Sci. **20**, 66 (1992).
[16] I. D. Kaganovich and L. D. Tsendin, IEEE Trans. Plasma Sci. **20**, 80 (1992).
[17] K. E. Orlov and A. S. Smirnov, Plasma Sources Sci. Technol. **8**, 2194 (1999).
[18] S. H. Seo, J. I. Hong, K. H. Bai, and H. Y. Chang, Phys. Plasmas **8**, 614 (1999).
[19] O. V. Polomarov, C. E. Theodosiou, I. D. Kaganovich, D. J. Economou, and B. N. Ramamurthi, IEEE Trans. Plasma Sci. **34**, 767 (2006).